Short Communication

Electrochemical Immunoassay Analysis of Apolipoprotein A for Potential Diagnosis of Coronary Artery Disease

Lei Liu, Xianen Fa[*]*, Yuyang Zhou, Chengshan Gao and Haibin Yu*

Department of Cardiovascular Surgery, The Second Affiliated Hospital of Zhengzhou University, Zhengzhou, Henan, 450052, P.R. China
[*]E-mail: 3419543778@qq.com

The development of sensitive detection method for human apolipoprotein A (Apo-A) that is an important marker for coronary artery disease is highly demanded. In this study, a uniform composite composed of chemically reduced graphene (GR) and multi-walled carbon nanotubes (MWCT) was prepared via layer-by-layer assembly method. Cyclic voltammetry (CV) and electrochemical impedance spectroscopy (EIS) were employed for investigating the electrochemical performance of GR-MWCT modified electrode. The content of Apo-A could be determined according to the change of reductive current after the electrode was functionalized with HRP-labeled Apo-A antibody. The current response of proposed immunosensor fabricated with GR-MWCT modified electrode was related linearly with the logarithm of human Apo-A concentration within the range of 0.5-1000.0 ng/mL. The detection limit of Apo-A immunosensor was 0.2 ng/mL (S/N=3). In addition, the proposed immunosensor showed excellent specificity for the detection of human Apo-A. In general, the Apo-A immunosensor with remarkable performance demonstrated huge potential use in the clinic diagnosis of coronary artery disease.

Keywords: Coronary artery disease; Apolipoprotein A; Immunoassay; Electrochemistry; Carbon nanomaterials

1. INTRODUCTION

The occurrence of atherosclerotic cardiovascular diseases (ASCVD) is implicated with both fasting hypertriglyceridaemia and postprandial hyperlipidaemia (PH) [1, 2]. As shown by considerable research [3, 4], PH is normally caused by the postprandial accumulation of triglyceride (TG) which is rich lipoproteins and its partial hydrolysis products, namely remnant lipoproteins. Actually, the incidence of coronary artery disease (CAD) is closely related with the level of remnant lipoprotein

cholesterol [5, 6]. Recently, the atherogenicity of remnant lipoproteins has aroused general concern. However, less research has been paid on the atherogenicity of chylomicron remnants (CM-R) than that of intermediate-density lipoprotein (IDL) and very-low-density lipoproteins remnants (VLDL-R). An assay system has been developed for the measurement of serum apolipoprotein A (Apo-A) concentration which is a representation of chylomicrons (CMs) and CM-R content in serum [7]. Compared with healthy people, the concentration level of Apo-A ranging from 0 to 25 μg/mL with the mean ± SD value of 5.2 ± 3.8 μg/mL is significantly higher in patients with hyperlipidaemic and metabolic syndrome (MetS) owing to the accumulation of CMs and CM-R [8].

Electrochemical immunoassay has been widely used in the clinical determination of biomarkers because of its easy operation and high sensitivity [9, 10]. Owing to the specific immunoreaction between antibody and antigen on the surface of proposed electrode, electrochemical immunoassay demonstrates remarkable selectivity in the detection of analyte. Nevertheless, conventional antibody is customarily unstable, leading to the requirement of scrupulous and careful preparation. Recently, nanobodies (Nbs) that are variable domains of heavy-chain antibodies (VHHs) have attracted wide attention in the development of electrochemical immunosensors owing to its better binding specificity with smaller size in comparision with conventional monoclonal antibodies [11, 12]. In addition, immunosensors that constructed with Nbs exhibit excellent stability due to the good thermal and chemical stability of Nbs. Nevertheless, the studies on Nbs are still limited, and the existing few researches were mainly focused on the application in drug development. Recently, a pair of Nbs (Nb11 and Nb19) was screened out from Bactrian camels for the first time. The new-found Nbs could be employed to fabricate electrochemical immunosensor for the detection of Apo-A1 owing to its ability to combine with different epitopes of Apo-A1 to form a sandwich-type immunocomplex.

The performance of electrochemical immunosensors is closely related with mass transport and electron transfer of biomolecule activities which is greatly affected by the properties of electrode interface such as structure, BET surface area, conductivity and biocompatibility [9, 13-16]. In addition, the stability of proposed biosensors is very much a function of the strong interaction between biomolecule activities and electrode interface [17]. Recently, nanomaterials with numerous advantages such as excellent electrical conductivity and biocompatibility, high BET surface area and remarkable electrocatalytic activity have demonstrated promising potential in the application of constructing intelligent multifunctional electrochemical interface of high performance electrochemical immunosensors [18-21].

Carbon nanomaterials with remarkable physical properties have high value and huge potential use in the development of electrochemical biosensors. As a star member of carbon nanomaterials, carbon nanotubes with quasi-one dimensional (1D) structure assembled by rolling graphite sheets have been widely used for fabricating electrochemical biosensors owing to excellent electrical conductivity, outstanding mechanical and chemical stability [14, 22-24]. As another new carbon materials, graphene with fascinating two-dimensional (2D) structure has demonstrated electrocatalytic activity towards many substances including TNT, H_2O_2, NADH, dopamine and O_2 because of its large BET surface area and extraordinary electrochemical properties as well [25-27]. Chemically reduced graphene (GR) which can be prepared via chemical reduction of graphene oxide is easily functionalized to form nanostructure hybrid materials owing to the remaining functional groups including carboxyl, hydroxyl

and epoxy on the surface and edges. Subsequently, the as-prepared multifunctional hybrid materials demonstrate huge potential in the application of fabricating sensing or energy conversion devices with high efficiency [28, 29].

In this study, a layer-by-layer assembly method was employed for the fabrication of composite electrode interface that was composed of multi-walled carbon nanotubes (MWCT) with quasi 1D structure and graphene with 2D plane structure. Specifically, the composite was synthesized via electrostatic adsorption between negatively charged MWCT and GR and positively charged poly(diallyldimethylammonium chloride) (PDDA). Cyclic voltammetry and electrochemical impedance spectroscopy (EIS) were applied for investigate the electron transfer performance of as-prepared electrode. In addition, a nanobody-based electrochemical immunoassay was fabricated with the as-prepared MWCTs and GR modified electrode for the detection of protein Apo-A. The proposed immunosensor demonstrated promising potential use in the diagnosis of coronary artery disease owing to the observed excellent detection performance toward Apo-A in human serum.

2. EXPERIMENTS

Graphite powder (99.99995%, 325 mesh), N-hydroxylsuccinimide (NHS), horse reddish peroxidase (HRP), 1-ethyl-3-(3-dimethylaminopropyl) carbodiimide hydrochloride (EDC), hydroquinone (HQ), quinine (Q), H_2O_2 (30%) and bovine serum albumin (BSA) were obtained from Alfa Aesar. Poly(diallyldimethylammonium chloride) (PDDA) with the molecular weight of about 100,000 was supplied by Sigma-Aldrich and used as received. Human Apo-A, Human Apo-A antibody and HRP labeled human Apo-A antibody were purchased from Abcam (Hong Kong) Ltd. All other chemicals were analytic reagents and purchased directly. Ultrapure water (Milli-Q, 18.2 MΩ cm) was used throughout all experiments.

A glassy carbon electrode (GC) with diameter of 3 mm was firstly polished with 1.0, 0.3, and 0.05 μm α-Al_2O_3 powder and then washed with ethanol and water under ultrasonic before use. Subsequently, the treated GC electrode was immersed in a PDDA aqueous solution (10 mg/mL) containing NaCl (20 mM) for 30 min. Finally, the GC electrode was washed with distilled water and then dried with flow nitrogen. In order to achieve GR modified electrode, the PDDA modified GC electrode was further immersed in a GR dispersed solution with the concentration of 1 mg/mL for 30 min. Subsequently, the electrode was immersed again in PDDA solution for 30 min. In order to achieve MWCTs modified electrode, the electrode was then immersed into MWCTs dispersed solution with the concentration of 1 mg/mL for 30 min after the drying step. A stable GR/MWCNT electrode was successfully prepared by repeating the above procedures three times. The as-prepared composite electrode was firstly rinsed with ultrapure water for 10 min before the further immobilization of antibodies, and then the GR/MWCNT electrode was incubated in human Apo-A antibody solution with the concentration of 100 μg/mL for 2 h. In order to block the non-specific binding sites, BSA solution with the concentration of 1 mg/mL was employed. Then the modified electrode was incubated in Apo-A solution with specific concentration for 1.5 h. Finally, HRP-labeled human Apo-A antibodies (50 μg/mL) were dropped onto the surface of modified electrode and the reaction lasted for

1.5 h. Each incubation procedure was carried out at 37 °C and PBS (0.01 M) was used to wash the electrode surface for 10 min after each step.

A conventional three-electrode system with human Apo-A antibody immobilized GR/MWCNT electrode, Ag/AgCl electrode and platinum slice (1×2 cm^2) as working, reference and counter electrodes, respectively, was used for all electrochemical experiments. Amperometric measurements of electrochemical immunoassay were carried out under stirring with -0.08 V as working potential and 30 mL of hydroquinone containing PBS buffer solution (1 mM) as electrolyte. Subsequently, 200 μL of H_2O_2 (1 mM) was quickly added to the above solution at the point of steady-state value of transient currents achieved. When proteins BSA and Apo-A existed simultaneously, the selectivity of constructed sensor could be obtained. All electrochemical experiments were performed at room temperature.

3. RESULTS AND DISCUSSION

Cyclic voltammetry (CV) curves of GR/MWCTs modified electrode were measured with 5 Mm $Fe(CN)_6^{4-/3-}$ in 0.1 M KCl solution as redox probe and 100 mV/s as scan rate. As shown from Fig. 1A, a couple of quasi-reversible redox peaks of $Fe(CN)_6^{4-/3-}$ were observed on bare GC electrode (curve a). The amperometric response of GR/MWCT modified GC electrode exhibited a marked increase in comparision with that of bare GC electrode (curve d), which could be resulted from the enhanced mass and electron transfer of $Fe(CN)_6^{4-/3-}$ions on the interface of electrode owing to the remarkable physical properties of GR and MWCTs. In addition, the increased surface area of electrode ascribed to GR and MWCTs plays an important role on the electrochemical performance of GR/MWCT modified GC electrode as well. It was found that the peak current obtained on MWCT (curve b) or graphene (curve c) modified GC electrode also increased compared with that obtained on bare GC electrode, which could be ascribed to the large BET surface area and outstanding electric conductivity of carbon nanomaterials. Nevertheless, the peak current of electrode modified GR-MWCT composite was higher than that of MWCT or graphene modified electrode, suggesting the synergistic action of GR and MWCT. The result demonstrates that the GR–MWCT composite electrode has superior electrochemical performances to those modified with MWCT or graphene individually [30, 31].

Electrochemical impedance spectra (EIS) were measured herein to investigate the impedance change of electrode during the modification process. Experiments were carried out in 0.1 M KCl solution with 5 Mm $Fe(CN)_6^{4-/3-}$ as redox probe, and the used frequency range was between 0.1 Hz and 10^5 Hz with signal amptitude of 5 mV. The obtained Nyquist plot is composed of semi-circle at high frequency range that corresponds to electron transfer-limit process and straight line at low frequency range that corresponds to diffusion-limit process. The electron transfer resistance as an indicator of electron transfer kinetics of electroactive probe can be calculated from the diameter of semi-circle. The measured Nyquist plots of bare GC electrode, GR, MWCT and GR-MWCT composite modified GC electrode were shown in Fig. 1B, respectively. Obviously, the electron transfer resistance of modified electrode exhibited a decrease. In addition, the diameter of semi-circle obtained

on electrode modified with GR-MWCT composite was smallest, suggesting that the electron transfer resistance at the interface of electrode was greatly reduced by GR-MWCT composite. The obtained results were consistent with that obtained from CV curves, confirming the positive effect of as-prepared GR-MWCT composite on the improvement of interfacial electron transfer. It was speculated that the electron transfer was greatly improved owing to the 3D direction pathway for electron moving in GR-MWCT composite, in contrast to the 2D and 1D direction pathway in graphene and MWCT modified electrodes, respectively.
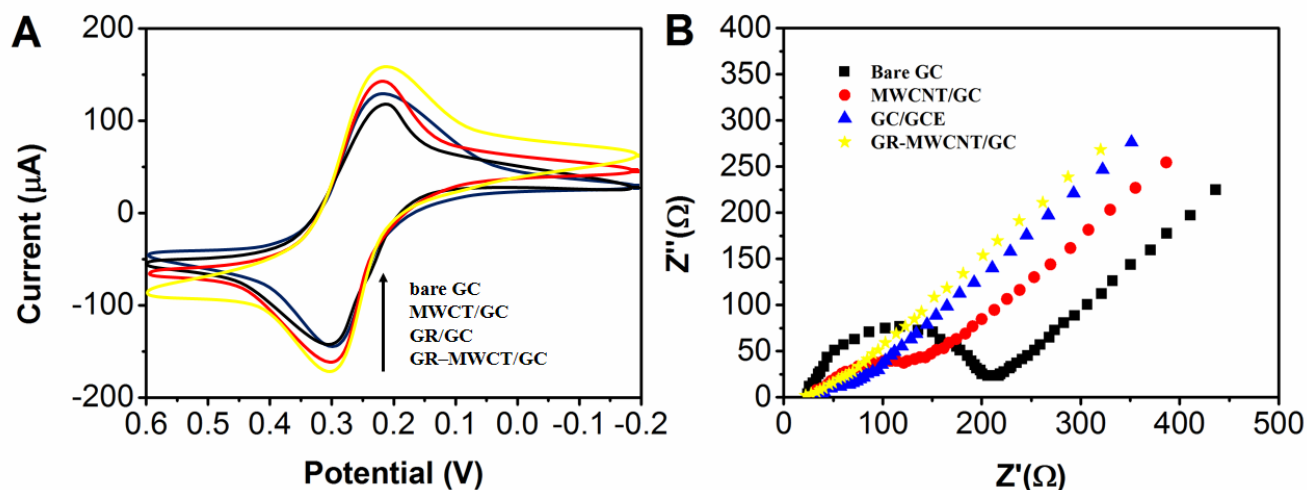
Figure 1. (A) Cyclic voltammograms and (B) electrochemical impedance spectra of bare GC, MWCT/GC, GR/GC and GR-MWCT/GC electrodes.

Cyclic voltammograms (CVs) curves of as-prepared electrodes were also measured in 0.01 M PBS solution (pH 7.4) containing enzymatic substrate 1 mM HQ and 1 mM H_2O_2 and the results were shown in Fig. 2. Apo-A with different concentrations were added into the above-mentioned solutions. As can be seen from the obtained CVs, a well-defined reduction peak was observed at -0.08 V. It was worth noting that the response current increased with increasing Apo-A concentration, which was resulted from more HRP labeled human Apo-A antibody captured at electrode surface due to higher Apo-A concentration, leading to the increase of reduction peak current in the presence of HQ and H_2O_2. The GR-MWCT serve as the carrier of human Apo-A antibody, Apo-A and the HRP labeled Apo-A anti-body. In the presence of H_2O_2, the HRP molecules catalyze the oxidation of HQ and the reductive current in this process can be recorded. According to this principle, the changes in the electrochemical signal (reductive current) could be used to detect Apo-A quantitatively [32, 33].

The GR-MWCT/GC electrode acts as the carrier for Apo-A, human Apo-A antibody and HRP labeled Apo-A antibody. In the presence of H_2O_2, hydroquinone (HQ) could be oxidized to quinine (Q) by HRP molecules and the reductive current during the process was recorded. Thus, the content of Apo-A could be determined according to the change of reductive current.
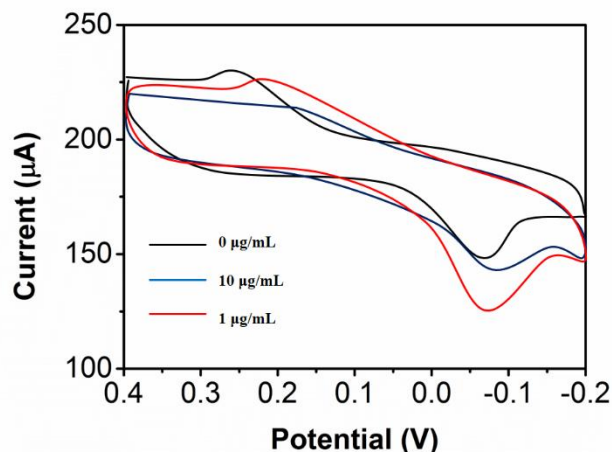
Figure 2. CVs of as-prepared immunosensor with Apo-A at different concentrations. The red dash line represents the reduction potential of H_2O_2 at -0.08 V.

Chronoamperometry was employed to monitor the current change (ΔI) in function of human Apo-A concentration. The experiments were carried out in 0.01 M PBS containing 1 mM hydroquinone and 1 mM H_2O_2. Before the electrochemical experiments, both the concentration of Apo-A antibody and HRP-labeled Apo-A antibody were optimized with immobilization efficiency as the criterion and the optimized values were 100 μg/mL and 50 μg/mL, respectively. As shown from Fig. 3A, the amperometric current of immunosensor constructed with GR-MWCT/GC electrode reached a plateau rapidly. As can be seen from Fig. 3C, amperometric response (ΔI) was related linearly with logarithm of human Apo-A concentration within the range of 0.5-1000 ng/mL. In addition, small error bars with the relative standard deviation (RSD) of 3.5% was observed, indicating the excellent sensor reproducibility of proposed sensor. The detection limit of electrochemical immunosensor constructed with GR-MWCT/GC electrode for the determination of human Apo-A is 0.2 ng/mL (*S*/*N*=3), suggesting that our proposed electrochemical immunosensors demonstrated huge potential use in the clinical diagnose since the concentration of Apo-A is typically around μg/mL range in cerebrospinal fluid for the patients carrying Apo-A in physiological conditions. The sensitivity of the proposed sensor was compared with that of other reported Apo sensors and the results were presented in Table 1.

Table 1. Comparison of the present electrochemical sensor with other Apo determination methods.

Method	Target	Linear detection range	Detection limit	Reference
DHPLC	Apo-E	—	—	[34]
ELISA	Apo-B	2.5-5.56 μg/mL	—	[35]
ELSA	Apo-B	0.903-1.09 μg/mL	0.084 μg/mL	[36]
MS	Apo-A	0.5–250 ng/mL	0.2 ng/mL	[37]
GR-MWCT/GC	Apo-A	0.5-1000 ng/mL	0.2 ng/mL	This work
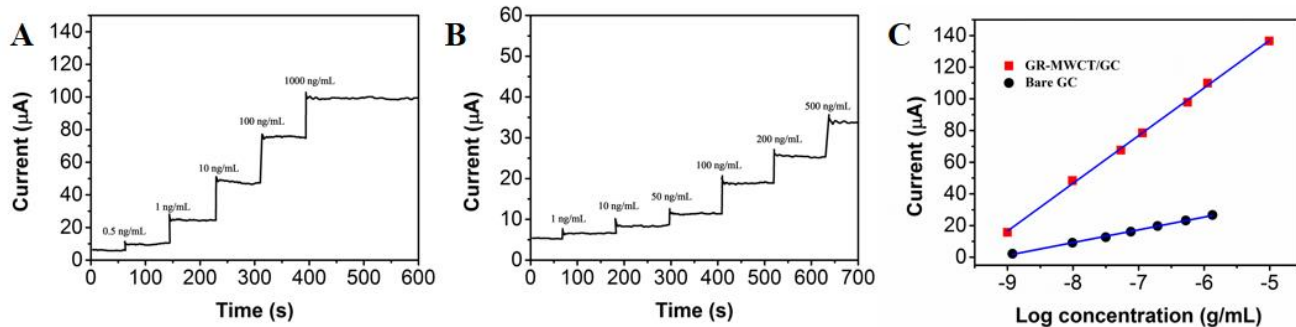
Figure 3. Amperometric results for (A) GR-MWCT/GC electrode and (B) bare GC electrode constructed electrochemical immunosensor incubated with different concentrations of human Apo-A protein in the range of 0.5-1000 ng/mL. (C) The calibration plots of amperometric response in function of logarithm of human Apo-A concentration.

As shown from Fig. 3B, the amperometric response of immunosensors constructed with bare GCE electrode exhibited a 60% decrease in comparision with that of immunosensor constructed with GR-MWCT electrode. In addition, the detection limit of immunosensor constructed with bare GC electrode for Apo-A (1 ng/mL) was higher than that of immunosensor constructed with GR-MWCT electrode (0.2 ng/mL), indicating that the GR-MWCT electrode was much more sensitive to Apo-A than bare GC electrode. Based on previous studies [38-40], the electroactive surface area could be calculated by measuring CV curves in 0.5 M H_2SO_4. It was found that the measured electroactive surface area of GR-MWCT/GC was larger than that of bare GC electrode, which was highly beneficial to the enhancement of active recognition sites. In addition to the increase of surface area, 3D porous nanostructures of GR-MWCT/GC were also significantly important to the improved accessibility of analytes to electrode surface by the shorter diffusion distance and the enhanced binding efficiency.
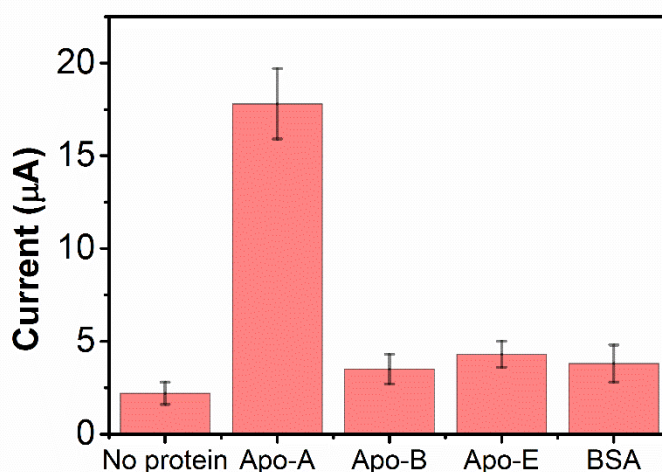
Figure 4. Current responses of as-prepared Apo-A electrochemical immunosensors for the detection of different analytes (0.5 μg/mL Apo-A, 1 μg/mL BSA, 1 μg/mL Apo-B and 1 μg/mL Apo-E). The error bars represent the standard deviation calculated with three independent experiments.

The specificity of the proposed electrochemical immunosensor to Apo-A was also investigated. As shown from the current response recorded in the presence of BSA (1 µg/mL), human Apo-E (1 µg/mL), human Apo-B (1 µg/mL) and human Apo-A (0.5 µg/mL) (Fig. 4), only human Apo-A demonstrated an obvious current response even though the concentration of Apo-A was lower than that of other proteins. The ΔI for the determination of BSA, Apo-B and Apo-E are 3.44%, 5.28%, and 7.85% of that for the determination of human Apo-A, respectively, suggesting the excellent specificity of as-prepared electrochemical immunosensor for the detection of human Apo-A.

4. CONCLUSIONS

In conclusion, a uniform GR-MWCT composite modified electrode was successfully prepared via layer-by-layer assembly method. The as-synthesized GR-MWCT composite with 3D porous structure exhibited remarkable electrochemical performance with significant improvement of mass and electron transfer owing to the high BET surface area and excellent electrical conductivity of GR and MWCT. A novel Apo-A electrochemical immunosensor was fabricated with GR-MWCT composite modified GC electrode. The binding efficiency between antigen and antibody was greatly improved owing to the large electroactive surface area and good biocompatibility of GR-MWCT/GC electrodes. The current response of electrochemical immunosensor was related linearly with logarithm of human Apo-A concentration within the range of 0.5-1000 ng/mL. In addition, the detection limit of proposed Apo-A electrochemical immunosensor fabricated with GR-MWCT/GC electrode is 0.2 ng/mL, which is better than that of immunosensor fabricated with bare GC electrode. What's more, the as-prepared electrochemical immunosensor demonstrated excellent specificity for the detection of human Apo-A.

References

1. J. Hokanson and M. Austin, *Journal of Cardiovascular Risk*, 3 (1996) 213.
2. H. Iso, Y. Naito, S. Sato, A. Kitamura, T. Okamura, T. Sankai, T. Shimamoto, M. Iida and Y. Komachi, *American Journal of Epidemiology*, 153 (2001) 490.
3. F. Karpe, *Journal of Internal Medicine*, 246 (1999) 341.
4. Y. Fujioka and Y. Ishikawa, *Journal of Atherosclerosis and Thrombosis*, 16 (2009) 145.
5. K. Kugiyama, H. Doi, K. Takazoe, H. Kawano, H. Soejima, Y. Mizuno, R. Tsunoda, T. Sakamoto, T. Nakano and K. Nakajima, *Circulation*, 99 (1999) 2858.
6. Y. Nakada, H. Kurosawa, J. Tohyama, Y. Inoue and K. Ikewaki, *Journal of Atherosclerosis and Thrombosis*, 14 (2007) 56.
7. N. Sakai, Y. Uchida, K. Ohashi, T. Hibuse, Y. Saika, Y. Tomari, S. Kihara, H. Hiraoka, T. Nakamura and S. Ito, *J. Lipid Res*, 44 (2003) 1256.
8. M. Kinoshita, H. Ohnishi, T. Maeda, N. Yoshimura, Y. Takeoka, D. Yasuda, J. Kusano, Y. Mashimo, S. Saito and K. Shimamoto, *Journal of Atherosclerosis and Thrombosis*, 16 (2009) 517.
9. G. Lai, F. Yan, J. Wu, C. Leng and H. Ju, *Anal. Chem.*, 83 (2011) 2726.
10. C. Zhu, G. Yang, H. Li, D. Du and Y. Lin, *Anal. Chem.*, 87 (2014) 230.
11. H. Li, Y. Mu, J. Yan, D. Cui, W. Ou, Y. Wan and S. Liu, *Anal. Chem.*, 87 (2015) 2007.
12. H. Li, Y. Sun, J. Elseviers, S. Muyldermans, S. Liu and Y. Wan, *The Analyst*, 139 (2014) 3718.
13. D. Chen, G. Wang and J. Li, *J. Phys. Chem. C.*, 111 (2007) 2351.
14. C.B. Jacobs, M.J. Peairs and B.J. Venton, *Anal. Chim. Acta.*, 662 (2010) 105.

15. X. Lu, Z. Wen and J. Li, *Biomaterials*, 27 (2006) 5740.
16. A. Warsinke, *Anal. Bioanal. Chem.*, 393 (2009) 1393.
17. D. Chen and J. Li, *Surf. Sci. Rep.,* 61 (2006) 445.
18. G. Jie, J. Zhang, D. Wang, C. Cheng, H. Chen and J. Zhu, *Anal. Chem.*, 80 (2008) 4033.
19. G. Jie, P. Liu, L. Wang and S. Zhang, *Electrochem. Commun.*, 12 (2010) 22.
20. S. Pinijsuwan, P. Rijiravanich, M. Somasundrum and W. Surareungchai, *Anal. Chem.*, 80 (2008) 6779.
21. Y. Wu, H. Shi, L. Yuan and S. Liu, *Chem. Commun.*, 46 (2010) 7763.
22. A. Ahammad, J. Lee and M. Rahman, *Sensors*, 9 (2009) 2289.
23. L. Bareket, A. Rephaeli, G. Berkovitch, A. Nudelman and J. Rishpon, *Bioelectrochemistry*, 77 (2010) 94.
24. Y. Liu, Y. Liu, H. Feng, Y. Wu, L. Joshi, X. Zeng and J. Li, *Biosens. Bioelectron.*, 35 (2012) 63.
25. F. Kong, M. Xu, J. Xu and H. Chen, *Talanta*, 85 (2011) 2620.
26. L. Lu, H. Li, F. Qu, X. Zhang, G. Shen and R Yu, *Biosens. Bioelectron.*, 26 (2011) 3500.
27. Y. Wang, Y. Li, L. Tang, J. Lu and J. Li, *Electrochem. Commun.*, 11 (2009) 889.
28. H. Bai, C. Li and G. Shi, *Adv. Mater.*, 23 (2011) 1089.
29. Y. Wan, Y. Wang, J. Wu and D. Zhang, *Anal. Chem.*, 83 (2010) 648.
30. B. Unnikrishnan, V. Mani and S. Chen, *Sens. Actuators, B.,* 173 (2012) 274.
31. V. Mani, A. Vilian and S. Chen, *Int J Electrochem Sci*, 7 (2012) 12774.
32. T.A. Silva, H. Zanin, F.C. Vicentini, E.J. Corat and O. Fatibello-Filho, *The Analyst*, 139 (2014) 2832.
33. S. Wang, W. Zhang, X. Zhong, Y. Chai and R. Yuan, *Analytical Methods*, 7 (2015) 1471.
34. Y. Zeng, F. Miao, L. Li, D. Sun and X. Xu, *Journal of Alzheimer's Disease*, 12 (2007) 357.
35. M. Kinoshita, M. Kojima, T. Matsushima and T. Teramoto, *Clin. Chim. Acta.*, 351 (2005) 115.
36. M. Kinoshita, T. Matsushima, Y. Mashimo, M. Kojima, M. Kigure and T. Teramoto, *Exp. Anim.,* 59 (2010) 459.
37. R. Silva, G. Hilliard, L. Li, J. Segrest and W. Davidson, *Biochemistry*, 44 (2005) 8600.
38. D. Nagaraju and V. Lakshminarayanan, *J. Phys. Chem. C.*, 113 (2009) 14922.
39. S. Trasatti and O. Petrii, *J. Electroanal. Chem.*, 327 (1992) 353.
40. L. Xu, S. Wang, H. Dong, G. Liu, Y. Wen, S. Wang and X. Zhang, *Nanoscale*, 4 (2012) 3786.